

Carrier-Induced Magnetic Circular Dichroism in the Magnetoresistive Pyrochlore $Tl_2Mn_2O_7$.

Hidekazu Okamura, Toshihisa Koretsune, Shin-ichi Kimura¹, Takao Nanba,
Hidetoshi Imai², Yuichi Shimakawa^{2,y} and Yoshinori Kubo²

Graduate School of Science and Technology, Kobe University, Kobe 657-8501

¹ UVSOR Facility, Institute for Molecular Science, Okazaki 444-8585

² Fundamental Research Laboratories, NEC Corporation, Tsukuba 305-8501.

(Received February 4, 2022)

Infrared magnetic circular dichroism (MCD), or equivalently magneto-optical Kerr effect, has been measured on the $Tl_2Mn_2O_7$ pyrochlore, which is well known for exhibiting a large magnetoresistance around the Curie temperature $T_C \approx 120$ K. A circularly polarized, infrared synchrotron radiation is used as the light source. A pronounced MCD signal is observed exactly at the plasma edge of the reactivity near and below T_C . However, contrary to the conventional behavior of MCD for ferromagnets, the observed MCD of $Tl_2Mn_2O_7$ grows with the applied magnetic field, and not scaled with the internal magnetization. It is shown that these results can be basically understood in terms of a classical magnetoplasma resonance. The absence of a magnetization-scaled MCD indicates a weak spin-orbit coupling of the carriers in $Tl_2Mn_2O_7$. We discuss the present results in terms of the microscopic electronic structures of $Tl_2Mn_2O_7$.

KEYWORDS: $Tl_2Mn_2O_7$, infrared magnetic circular dichroism, magnetoplasma, colossal magnetoresistance.

1. Introduction

Physics of colossal magneto-resistance (CMR) phenomena has attracted much interest recently. The most famous examples are probably the ferromagnetic perovskite manganites such as $La_{1-x}Sr_xMnO_3$.¹ In these compounds, the so-called "double exchange" interaction and the strong Jahn-Teller effect due to Mn^{3+} are responsible for the CMR and other interesting properties near the Curie temperature (T_C).^{2,3} Another CMR compound that is equally interesting is the $Tl_2Mn_2O_7$ pyrochlore.⁴⁻⁹ This compound is also a ferromagnet, and its resistivity (ρ) drops rapidly upon cooling below $T_C \approx 120$ K. Near and above T_C , an external magnetic field (B) of 7 T reduces ρ by a factor of ~ 10 . Although these features appear similar to those for the perovskites, it has been shown that the underlying mechanism is very different: The spontaneous magnetization below T_C is produced by the Mn^{4+} sublattice through superexchange interaction, independently from the conduction electrons. The conduction band has large Tl 6s and O 2p components.^{8,10,11} The CMR mainly results from changes in the conduction band when the applied B field induces a magnetization and hence a band polarization. Such magneto-resistance mechanism has been considered^{12,13} to be analogous to that of europium chalcogenides such as EuO .

Our previous magneto-optical study of $Tl_2Mn_2O_7$ provided much information regarding its electronic structures.¹⁴ The optical reactivity spectrum $R(\omega)$ at 295 K was similar to those for insulating oxides. Upon cooling below T_C , however, $R(\omega)$ showed marked increases in the far-infrared region, with a clear plasma edge un-

dergoing blue shifts with decreasing temperature (T). These changes clearly indicated a crossover to metallic electronic structures below T_C . $R(\omega)$ also showed large increases and plasma edge shifts when a strong magnetic field was applied near T_C , that were very similar to those caused by cooling. Based on the $R(\omega)$ data and the optical conductivity ($\sigma(\omega)$) obtained from $R(\omega)$, we concluded that the CMR was caused by the appearance of a small conduction band, and that the B -induced changes in the electronic structure were very similar to those induced by cooling at $B = 0$. It was also found that the effective carrier density showed a universal scaling with M^2 , where M is the internal magnetization, over wide ranges of T and B .

In this work we have studied the magnetic circular dichroism (MCD) of $Tl_2Mn_2O_7$ in order to obtain information about spin-dependent carrier dynamics below T_C . An MCD refers to a magnetically-induced difference between the optical responses to the incident light with right- and left-circular polarizations. In principle it can be a sensitive probe of spin-polarized electronic states in a magnetic material. Band calculations for ferromagnetic $Tl_2Mn_2O_7$ have predicted that the conduction electrons are completely spin-polarized.^{8,10,11} The carrier dynamics of such spin-polarized material is very interesting from both physical and technological points of view. A strong MCD has been observed exactly at the plasma edge of $R(\omega)$ in the infrared region, showing that the MCD arises from a small density of free carriers. The appearance of the MCD is closely related to the applied B , rather than M . We show that the observed MCD spectra can be basically understood based on a classical magneto-plasma model. The results are analyzed in terms of the electronic structures of $Tl_2Mn_2O_7$.

E-mail: okamura@phys.scikobe-u.ac.jp

^y Present Address: Institute for Chemical Research, Kyoto University, Uji 611-0011.

2. Experimental

We used the same TiMn_2O_7 sample, having $T_C = 120\text{ K}$, as that used in the previous report.¹⁴ The MCD experiments were done using a circularly polarized infrared synchrotron radiation as the light source, at the beam line BL6A1 of the UVSOR Facility, Institute for Molecular Science.^{15,16} Using synchrotron radiation source, one can obtain circularly polarized light over a wide range of photon energy,^{15,17} without additional optical elements such as a $\lambda/4$ plate. The reflectivity spectra of the sample were measured under a near-normal incidence, with magnetic fields applied perpendicular to the sample surface. An MCD under this condition is often referred to as the magneto-optical Kerr effect.¹⁸ The incident light always had right circular polarization, and the magnetic field was applied either parallel (B_+) or antiparallel (B_-) to the incident light. In this work we define the MCD spectrum as

$$M(\omega) = \frac{R_+(\omega) - R_-(\omega)}{R_{\text{avg}}(\omega)}; \quad (1)$$

where $R_{\pm}(\omega)$ are the $R(\omega)$ spectra measured under B_{\pm} fields, respectively, and $R_{\text{avg}}(\omega)$ is the average of $R_{\pm}(\omega)$. Namely the MCD is the relative difference in $R(\omega)$ that results when the B direction is reversed for a fixed helicity of circularly polarized incident light. (This is equivalent to reversing the helicity of the circular polarization for a fixed B direction.) The MCD thus defined is directly related to the Kerr ellipticity, $\kappa(\omega)$, as $\kappa(\omega) = \frac{1}{2} \theta_K(\omega)$.¹⁸ The Kerr rotation angle $\theta_K(\omega)$ is given as

$$\theta_K(\omega) = [\phi_+(\omega) - \phi_-(\omega)]/2; \quad (2)$$

Here $\phi_{\pm}(\omega)$ are the phase shifts of the complex reflectivity under B_{\pm} fields, which can be obtained from the $R_{\pm}(\omega)$ spectra using the Kramers-Kronig (K-K) relations.¹⁹ A superconducting magnet was used to apply the field, and a Fourier-transform interferometer was used to record the reflectivity spectra. The magneto-optical spectra were taken at photon energies below 1.1 eV , to which the zero-field spectra up to 35 eV ¹⁴ were smoothly connected.

3. Results and Discussion

Figure 1 shows the $R_{\text{avg}}(\omega)$ and the MCD spectra of TiMn_2O_7 at 40 K for $B = 2, 4$, and 6 T . $R_{\text{avg}}(\omega)$ at 40 K shows only minor dependence on B ,¹⁴ and the $R_{\text{avg}}(\omega)$ spectra at 0 and 6 T in Fig. 1 are almost unchanged. The sharp minimum in $R_{\text{avg}}(\omega)$ near 0.17 eV is the plasma edge, below which the reflectivity is high due to the Drude response of free carriers. The sharp structures in $R_{\text{avg}}(\omega)$ below 0.08 eV are due to optical phonons. As shown in the bottom graph of Fig. 1, a clear MCD is observed around the plasma edge, which becomes stronger with increasing B . The sharp MCD peaks around 0.05 eV probably result from the plasmon-LO phonon coupling,²⁰ which will not be discussed in this work. The Kerr rotation $\theta_K(\omega)$ at 6 T is also shown in Fig. 1. It is seen that the maximum Kerr rotation of TiMn_2O_7 is about 1° at $B = 6\text{ T}$.

The temperature dependence of the observed MCD at $B = 6\text{ T}$ is shown in Fig. 2, together with the $R_{\text{avg}}(\omega)$ spectra at 0 and 6 T . The field-induced variations of $R_{\text{avg}}(\omega)$ at 125 K , near T_C , are very large. This is due to the increase of free carriers caused by the band polarization induced by the applied magnetic field,¹⁴ which is closely related with the CMR. Away from T_C , however, the field-induced changes in $R_{\text{avg}}(\omega)$ are very small. The observed MCD becomes stronger with decreasing T . In addition, the position of the MCD peak closely follows that of the plasma edge, as the latter undergoes blue shifts with decreasing T . This result strongly suggests that the observed MCD is closely related with the free carriers in TiMn_2O_7 . Note that the field-induced changes of $R_{\text{avg}}(\omega)$ are largest near T_C , but the MCD becomes largest at lower temperatures.

Figure 3 plots the magnitude (peak height) of the MCD as functions of magnetic field and temperature, with the measured magnetization (M) of the same sample. Note that M is induced even well above T_C under applied fields of 4 and 6 T . Figure 3 clearly shows that the variation of MCD does not closely follow that of M . This is most clearly seen at 40 K in Fig. 3(a), where M is almost saturated above 0.5 T although the MCD grows with increasing B even above 4 T . In addition, Fig. 3(b) shows that the MCD appears only below 160 K , which is coincident with a rapid increase of M with cooling. This result probably indicates that a well-defined conduction band can be established only below 160 K , although an induced M exists even at higher temperatures.

An MCD due to free carriers may arise through several mechanisms. In a ferromagnetic metal such as Gd , free carriers may lead to an MCD due to their skew scatterings caused by the internal M and a spin-orbit coupling.²¹ Also for paramagnetic metals, a large MCD at ω_p has been attributed to an exchange-enhanced splitting of the plasma edge.²² In these cases, the MCD should be proportional to the spin polarization of the carriers. This is in contrast to the present results, where the observed MCD is not scaled with the internal M . Another possibility is a plasma edge-enhancement of MCD,^{23,25} where a strong MCD is caused when a steep plasma edge is present and well separated in energy from the interband transitions. Although the $R(\omega)$ spectra of TiMn_2O_7 below T_C may satisfy both of these conditions,¹⁴ this mechanism does not seem consistent with the B -dependence of the MCD for TiMn_2O_7 . Interaction of the plasma resonance with interband transitions involving magnetic states²⁶ is also unlikely, since ω_p is far apart from the interband transitions, located above 2 eV .¹⁴ We show below that the classical magnetoplasma (MP) resonance,^{20,27} which is a coupled Drude-cyclotron response of free carriers under B field, can basically account for the observed MCD. In this model an MCD appears at the plasma edge due to its splitting into $\omega_p \pm \omega_c$, where ω_c is the cyclotron energy.

We take the z axis normal to the sample surface, and the polarization vectors lie in the xy plane. Then in the classical MP model for isotropic band electrons, the com-

ponents of the complex dielectric tensor are given as^{20,27}

$$\hat{\epsilon}_{xx} = 1 - \frac{\omega_p^2}{\omega(\omega + i\gamma)} \frac{(\omega_c^2 + \gamma^2)}{\omega_c^2} \quad (3)$$

$$\hat{\epsilon}_{xy} = \hat{\epsilon}_{yx} = \frac{\omega_p^2}{\omega(\omega + i\gamma)} \frac{i\omega_c}{\omega_c^2}; \quad (4)$$

where ω_p and ω_c are the plasma and cyclotron energies, respectively, and γ is the damping. The complex refractive indices for $\hat{\epsilon}$ directions, \hat{N} , are the two eigenvalues of the complex refractive index tensor.¹⁸ They satisfy $\hat{N}^2 = \hat{\epsilon}_{xx} - \hat{\epsilon}_{xy}$. By definition, they also satisfy $\hat{N}^2 = \hat{\epsilon} = \epsilon_1 + i\epsilon_2$, where $\hat{\epsilon}$ are the complex dielectric functions of the MP for the $\hat{\epsilon}$ directions, and ϵ_1 and ϵ_2 are their real and imaginary parts, respectively. Hence we have

$$\hat{\epsilon}_{xx} - i\hat{\epsilon}_{xy} = \epsilon_1 + i\epsilon_2; \quad (5)$$

Substituting (3) and (4) into (5), we obtain

$$\epsilon_1 = 1 - \frac{\omega_p^2}{\omega^2 + \gamma^2} - \frac{\omega_p^2 \omega_c (\omega^2 - \gamma^2)}{\omega(\omega^2 + \gamma^2)^2} \quad (6)$$

$$\epsilon_2 = \frac{\omega_p^2}{\omega(\omega^2 + \gamma^2)} - \frac{2\omega_p^2 \omega_c}{(\omega^2 + \gamma^2)^2}; \quad (7)$$

where we have used ($\omega_c = \omega_p$) = 1, valid for the present case. The total dielectric function is expressed as¹⁹

$$\epsilon^t = \epsilon + \epsilon^{ib} + \epsilon^{ph}; \quad (8)$$

where ϵ^{ib} arises from the higher-energy interband transitions, which partially screens the plasma oscillations, and ϵ^{ph} arises from the optical phonons. $R(\omega)$ are given as¹⁹

$$R(\omega) = \frac{(n^2 - 1)^2 + k^2}{(n^2 + 1)^2 + k^2}; \quad (9)$$

where n and k are real and imaginary refractive indices, respectively, obtained by solving $\epsilon_1 = n^2 - k^2$ and $\epsilon_2 = 2nk$. Finally, the MCD in this model is obtained by substituting (9) into (1).

We simulate the observed MCD spectra using the above model as follows. First, we obtained the Dude parameters and ω_p by fitting the observed $R_{avg}(\omega)$ based on the regular Dude reactivity, i.e., that obtained by setting $\omega_c = 0$ in (6)–(9). In doing so, we also used the classical Lorentz oscillator model¹⁹ for the phonon part $\epsilon^{ph}(\omega)$, and the actual $\epsilon^{ib}(\omega)$ obtained from the measured $R_{avg}(\omega)$ through the K-K relations.²⁸ The observed $R_{avg}(\omega)$ spectra could be fitted well by this procedure, as shown in Fig. 4 (left axis). Then, we substituted the obtained ω_p and ω_c into (6)–(9), and adjusted ω_c as a parameter so that the MCD calculated through (1) reproduces the observed MCD spectrum. The fitted value of ω_c was used to calculate the effective mass m^* , using the relation $\omega_c = eB_1/m^*c$. Here, we have assumed that the internal field B_1 acting on the electrons is equal to the applied field.²⁹ Figure 4 shows the simulated reactivity and MCD spectra at 6 T, with the used parameters shown in the caption, and Fig. 5 plots the obtained m^* values at different values of B and T . The simulated spectra in Fig. 4 have well reproduced the observed MCD spectra in Fig. 2, with the obtained $m^* = m_0$ values of

0.8 at 4 T, and 0.6 at 6 T. These values are very reasonable, since they are close to those predicted by the band calculations for ferromagnetic $Tl_2Mn_2O_7$,^{8,10,11} and also to those estimated previously from the effective carrier density.¹⁴ Since the parameters ω_p and ω_c have been chosen to reproduce $R_{avg}(\omega)$, the only free parameter in simulating the MCD is m^* . Considering this fact and the simplicity of the model, the agreement between the data and the simulation is remarkable. The decrease in m^* from $B = 4$ T to 6 T is likely to result from changes in the band structure caused by the increase of M . In contrast, m^* does not show significant temperature dependence both at 4 and 6 T.

Regarding the field dependence of the MCD, there seems to be a threshold for the onset of MCD, as seen in Fig. 3(a): the MCD grows with B for 4 and 6 T, but is almost absent at 2 T. This is unexpected from the simple MP model, which predicts that the MCD at 2 T is about half that at 4 T. (Note that a well-defined conduction band exists for $T < T_c$ even at zero field.) The reason for this threshold behavior is unclear at the present, and it is likely to result from complications not included in the simple MP model. For example, the electrons experience scattering due to disorder such as defects and impurities, in addition to electron-phonon interaction. The degree of disorder-related scattering may vary with the field strength, depending on the relative magnitude of the magnetic length (cyclotron radius) to the spatial size of the disorder potential. Such scattering may make the contribution of cyclotron motion to the MP resonance observed only above certain field strength.

Our previous work¹⁴ has shown that the variations of $R(\omega)$ and $\epsilon(\omega)$ as functions of B and T closely follow the associated variations of the internal magnetization M . In fact, the effective carrier density evaluated from the measured spectra scaled with M^2 over wide ranges of T and B . In addition, the band calculations have predicted that the conduction electrons in $Tl_2Mn_2O_7$ are completely spin polarized. In view of these previous results, the absence of an M -scaled MCD for $Tl_2Mn_2O_7$ is a rather unexpected result. Since the angular momentum carried by a circularly polarized photon cannot directly couple with the electron spin and hence with M , the carriers must have a sufficient spin-orbit (s-o) coupling to lead to an MCD. Therefore the present result strongly suggests a weak s-o coupling for the conduction electrons in $Tl_2Mn_2O_7$. A weak s-o coupling of carriers in $Tl_2Mn_2O_7$ has also been indicated by the observation of a very weak anomalous Hall effect even well below T_c .⁹ According to the band calculations, the density of states for the conduction band below the Fermi level in ferromagnetic $Tl_2Mn_2O_7$ are mainly derived from the Tl 6s, O 2p, and Mn 3d states about 1:1:1 ratio. Among these, the orbital angular momentum for 3d electron is usually quenched, so that the O 2p component may be the only source of s-o coupling for the conduction electrons. This may account for the absence of an M -dependent MCD for $Tl_2Mn_2O_7$. For a more quantitative account of the observed MCD, however, it is probably necessary to take into account the actual band structures, as well as their dependence on the magnetization.

It is interesting to compare the present results of $T\frac{1}{2}Mn_2O_7$ with those of EuB_6 ,^{31,33} another ferromagnet with $T_C = 16$ K which shows large magneto-optical effects similar to those for $T\frac{1}{2}Mn_2O_7$. Near T_C , EuB_6 shows very large shifts of the plasma edge in $R(\theta)$ with T and B .^{31,32} The Drude weight (effective carrier density) scales with M^2 over wide ranges of T and B .³² A pronounced MCD appears at the plasma edge of $R(\theta)$, with a Kerr rotation angle as large as 8 degrees.³³ Although these results are qualitatively similar to those found for $T\frac{1}{2}Mn_2O_7$, there is one marked difference concerning the plasma edge MCD: In addition to the much larger magnitude, the MCD for EuB_6 follows the variation of M more closely than that for $T\frac{1}{2}Mn_2O_7$.³³ This is because the plasma edge MCD for EuB_6 is due to the spin polarization of the localized Eu 4f electrons under B fields, aided by the coupling between the Drude dynamics and the nearby interband transitions involving Eu 4f states.³³ This result is reasonable, since the Eu 4f electrons are directly responsible for the M . In contrast, in the case of $T\frac{1}{2}Mn_2O_7$ the source of MCD is the free carriers themselves, which have only small s - d coupling resulting in the absence of M -scaled MCD.

Conclusion

We have studied the infrared MCD (magneto-optical Kerr effect) of the magnetoresistive pyrochlore $T\frac{1}{2}Mn_2O_7$, using synchrotron radiation source. A pronounced MCD signal has been observed exactly at the plasma edge of the reflectivity. The observed MCD grows with the applied external magnetic field, and it is not scaled with the internal magnetization. The MCD has been successfully analyzed in terms of the classical magnetoplasma resonance model. The absence of strongly M -dependent MCD in $T\frac{1}{2}Mn_2O_7$ indicates a weak spin-orbit coupling of the conduction electrons in $T\frac{1}{2}Mn_2O_7$.

Acknowledgements

This work was performed as a joint studies program of the Institute for Molecular Science (2001). This work was partly supported by Grants-In-Aid from the MEXT.

- 1) See, for example, Y. Tokura, A. Uchishibara, Y. Morimoto, T. Arima, A. Asamitsu, G. Kido and N. Furukawa: J. Phys. Soc. Jpn. 63 (1994) 3931.
- 2) C. Zener: Phys. Rev. 82 (1951) 403.
- 3) A. J. M. Illis, P. B. Littlewood and B. I. Shraiman: Phys. Rev. Lett. 74 (1995) 5144.
- 4) Y. Shimakawa, Y. Kubo and T. Manako: Nature 379 (1996) 53.
- 5) M. A. Subramanian, B. H. Toby, A. P. Ramirez, W. J. Marshall, A. W. Sleight and G. H. Kwei: Science 273 (1996) 81.
- 6) S.-W. Cheong, H. Y. Hwang, B. Batlogg and L. W. Rupp, Jr.: Solid State Commun. 98 (1996) 163.
- 7) Y. Shimakawa, Y. Kubo, T. Manako, Y. V. Sushko, D. N. Argyriou and J. D. Jorgensen: Phys. Rev. B 55 (1997) 6399.
- 8) Y. Shimakawa, Y. Kubo, N. Hamada, J. D. Jorgensen, Z. Hu, S. Short, M. Nohara and H. Takagi: Phys. Rev. B 59 (1999) 1249.
- 9) H. Imai, Y. Shimakawa, Yu. V. Sushko and Y. Kubo: Phys. Rev. B 62 (2000) 12190.
- 10) D. J. Singh: Phys. Rev. B 55 (1997) 313.
- 11) S. K. Mishra and S. Satpathy, Phys. Rev. B 58 (1998) 7585.

- 12) Y. Shimakawa and Y. Kubo: Mater. Sci. Eng. B 63 (1999) 44.
- 13) M. Kataoka: Phys. Rev. B 63 (2001) 134435.
- 14) H. Okamura, T. Koretsune, M. Matsunagi, S. Kimura, T. Namba, H. Imai, Y. Shimakawa, Y. Kubo: Phys. Rev. B 64 (2001) 180409.
- 15) S. Kimura: Jpn. J. Appl. Phys. 38 Suppl. 38-1 (1999) 392.
- 16) S. Kimura, M. Okuno, H. Iwata, H. Kitazawa, G. Kido, F. Ishiyama, O. Sakai: J. Phys. Soc. Jpn. 71 (2002) 2200.
- 17) Actually, the incident light used was not completely circularly polarized, but elliptically polarized. However, the degree of circular polarization was estimated to be greater than 90%.¹⁵ Hence the uncertainty in the measured MCD caused by the incomplete circular polarization is less than 10%.
- 18) S. Sugano and K. Kojima (Eds.), Magneto-optics (Springer, Berlin, 2000).
- 19) M. Dressel and G. Grüner: Electrodynamics of Solids (Cambridge University Press, Cambridge, 2002).
- 20) R. W. Stiles and B. Lax: Phys. Rev. B 1 (1970) 4720.
- 21) J. L. Erskine and E. A. Stern: Phys. Rev. B 8 (1973) 1239.
- 22) W. Reim, O. E. Husser, J. Schoenes, E. Kaldis, P. Wächter and K. Seiler: J. Appl. Phys. 55 (1984) 2155.
- 23) H. Feil and C. Haas: Phys. Rev. Lett. 58 (1987) 65.
- 24) J. Schoenes and W. Reim: Phys. Rev. Lett. 60 (1988) 1988.
- 25) H. Feil and C. Haas: Phys. Rev. Lett. 60 (1988) 1989.
- 26) F. Salghetti-Drioli, P. Wächter and L. Degiorgi: Solid State Commun. 109 (1999) 773.
- 27) B. Lax and G. B. Wright: Phys. Rev. Lett. 4 (1960) 16.
- 28) In the measured spectra of $T\frac{1}{2}Mn_2O_7$, the interband transition peaks were well separated in energy from the Drude-Lorentz components.¹⁴ Hence $\epsilon_b(\omega)$ could be easily isolated from the measured total $\epsilon(\omega)$. The factor 1 in (5) was dropped since it should be included in $\epsilon_b(\omega)$.¹⁹
- 29) In the presence of a magnetization M , the internal field B_i may differ from the applied field B_0 , since M produces an additional field B_m , where $B_i = B_0 + B_m$. The detail of B_m depends on the sample shape and M . If there is a strong B_m in the $T\frac{1}{2}Mn_2O_7$ sample, this should appear, well below T_C , as a very rapid increase of the (ordinary) Hall voltage for $B_0 < 0.5$ T [see Fig. 3(a)], and it should scale with M rather than with B_0 . However, no such feature was observed in the experiments⁹ for a sample having similar shape as that used in the present work. In addition, for a wide, plate-shaped sample with M and B_0 perpendicular to the sample surface, it is well known that $B_i = B_0$. Our sample was a flat plate of $5 \times 5 \times 1$ mm³. From these facts, we believe that $B_i = B_0$ in our experiments.
- 30) The ϵ_p values obtained by fitting are much larger than the observed plasma edge positions in $R(\theta)$, since the fitted values are "bare" plasma energies while those observed in $R(\theta)$ have been reduced due to the screening by ϵ_b .
- 31) L. Degiorgi, E. Fekler, H. Rotter, J. L. Sarrao and Z. Fisk: Phys. Rev. Lett. 79 (1997) 5134.
- 32) S. Broderick, B. Ruzicka, L. Degiorgi, H. Rotter, J. L. Sarrao and Z. Fisk: Phys. Rev. B 65 (2002) 121102(R).
- 33) S. Broderick, L. Degiorgi, H. Rotter, J. L. Sarrao and Z. Fisk: Eur. Phys. J. B 33 (2003) 47.

Fig. 1. Top graph: the reactivity (R) spectrum of $\text{Ti}_2\text{Mn}_2\text{O}_7$ at $T = 40$ K and $B = 0$ and 6 T. Bottom panel: the MCD spectra, defined by (1), and the Kerr rotation θ_K measured at $T = 40$ K for $B = 2, 4$, and 6 T.

Fig. 2. Unpolarized reactivity spectra at magnetic fields 0 T (dotted curves) and 6 T (solid curves), and the MCD at 6 T (squares) of $\text{Ti}_2\text{Mn}_2\text{O}_7$ measured at four temperatures. MCD signals below 0.06 eV have been omitted for clarity.

Fig. 3. The magnitude of measured MCD (circles, squares, and triangles) plotted on the right axis as functions of (a) magnetic field and (b) temperature. The magnetization (M) of the sample is also plotted on the left axis (solid, dotted, and dashed-dotted curves).

Fig. 4. Simulated reactivity and MCD spectra at 6 T based on the MP model, as described in the text. The Druce parameters used are $(I_p, \gamma) = (0.24 \text{ eV}, 52 \text{ meV})$ for 140 K, $(0.325 \text{ eV}, 39 \text{ meV})$ for 125 K, $(0.38 \text{ eV}, 30 \text{ meV})$ for 100 K, and $(0.445 \text{ eV}, 30 \text{ meV})$ for 40 K. See also the note.³⁰

Fig. 5. Effective masses in units of the rest electron mass ($m^* = m_0$) obtained from the MCD data at magnetic fields $B = 4$ and 6 T as a function of temperature.

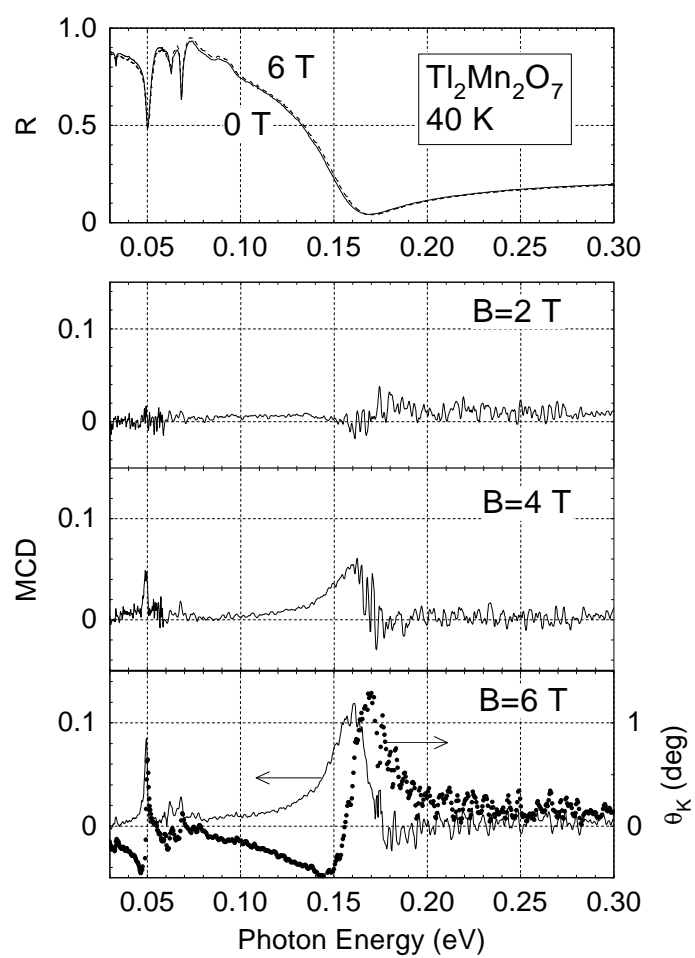


FIG.1
Okamura et al.

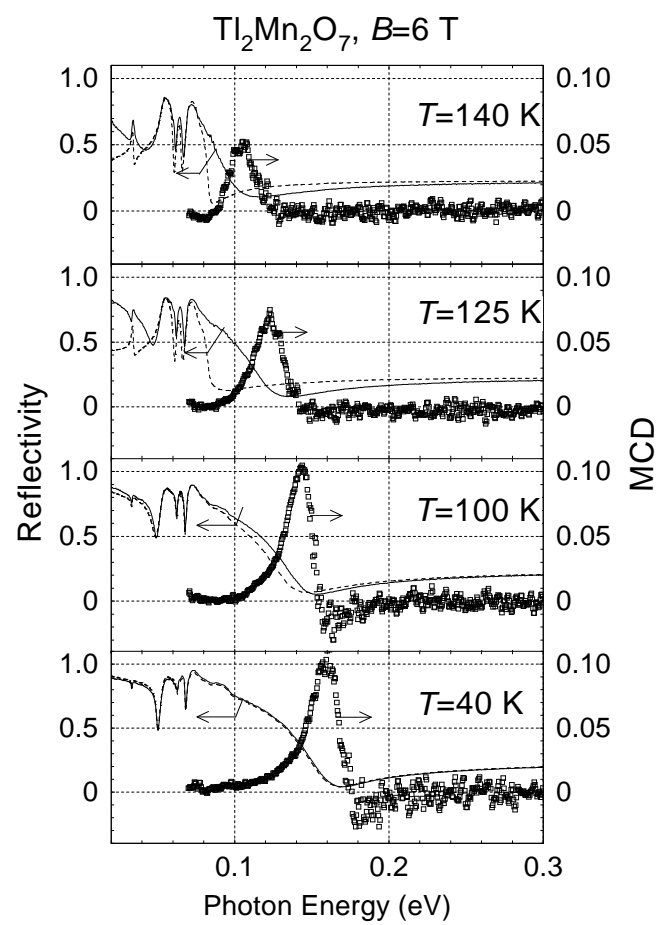


FIG.2
Okamura et al.

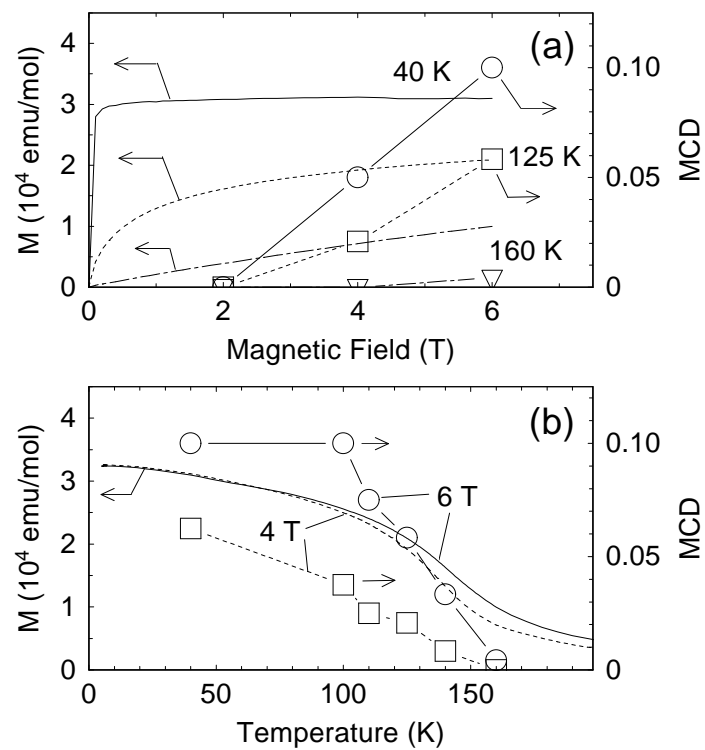


FIG.3
Okamura et al.

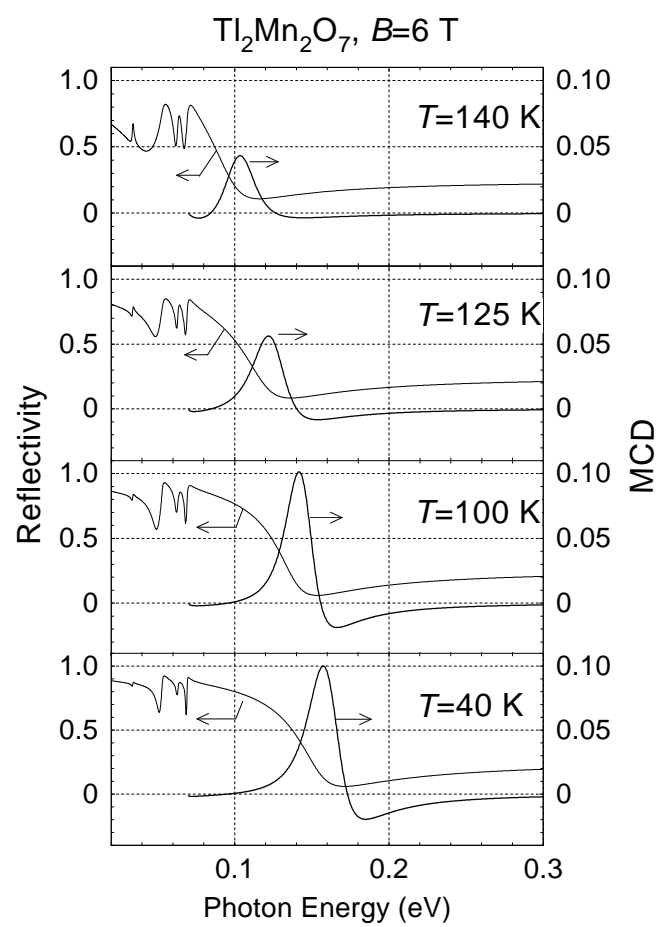


FIG. 4
Okamura et al.

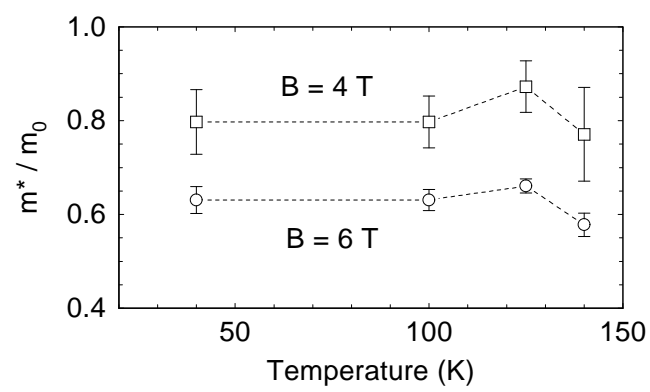


FIG.5
Okamura et al.